

ARTICLE

Supplementary Information

## High-efficiency, anode-free lithium-metal batteries with a close-packed homogeneous lithium morphology<sup>†</sup>

Laisuo Su,<sup>a</sup> Harry Charalambous,<sup>b</sup> Zehao Cui<sup>a</sup> and Arumugam Manthiram<sup>\*a</sup>

<sup>a</sup> Materials Science and Engineering Program & Texas Materials Institute, The University of Texas at Austin, Austin, TX 78712, United States.

<sup>b</sup> X-ray Science Division Advanced Photon Source, Argonne National Laboratory, 9700 S. Cass Avenue, Argonne Lemont, IL 60439, United States.

\*E-mail: manth@austin.utexas.edu

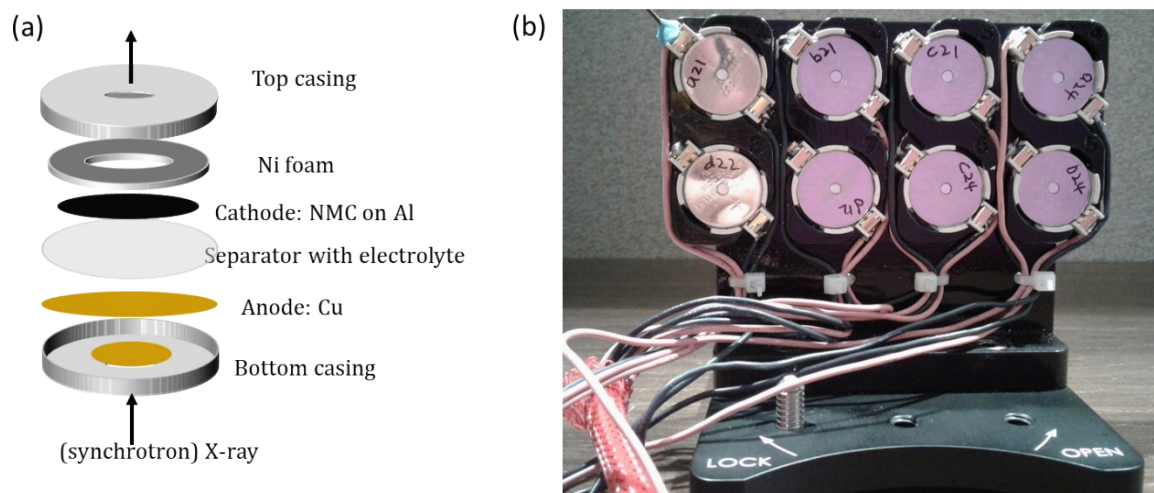


**Fig. S1** Operando XRD setup to monitor the kinetics of Li plating on Cu anode. (a) The components in a special designed window coin cell. (b) The coin cell holders for the operando experiment. The holder can take up to eight cells.

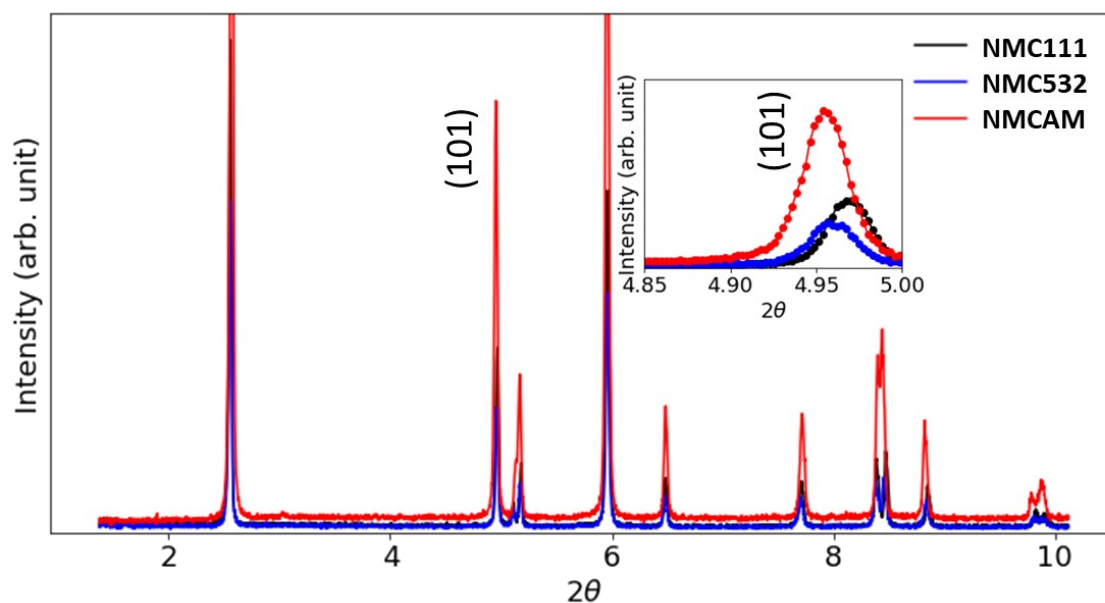


**Fig. S2** A comparison of the XRD pattern of  $\text{LiNi}_{1/3}\text{Mn}_{1/3}\text{Co}_{1/3}\text{O}_2$ ,  $\text{LiNi}_{0.5}\text{Mn}_{0.3}\text{Co}_{0.2}\text{O}_2$ , and  $\text{LiNi}_{0.95}\text{Mn}_{0.015}\text{Co}_{0.02}\text{Al}_{0.01}\text{Mg}_{0.005}\text{O}_2$  cathode materials with the X-ray energy of 56.2 keV. Inserted zooms in the  $2\theta$  region from  $4.85^\circ$  to  $5.00^\circ$ , where the Li (101) peak locates ( $4.88^\circ$ ). To avoid the interference between the (101) peak of the NMC cathode and the Li (101) peak, NMC111 is the best candidate among these three cathode materials.

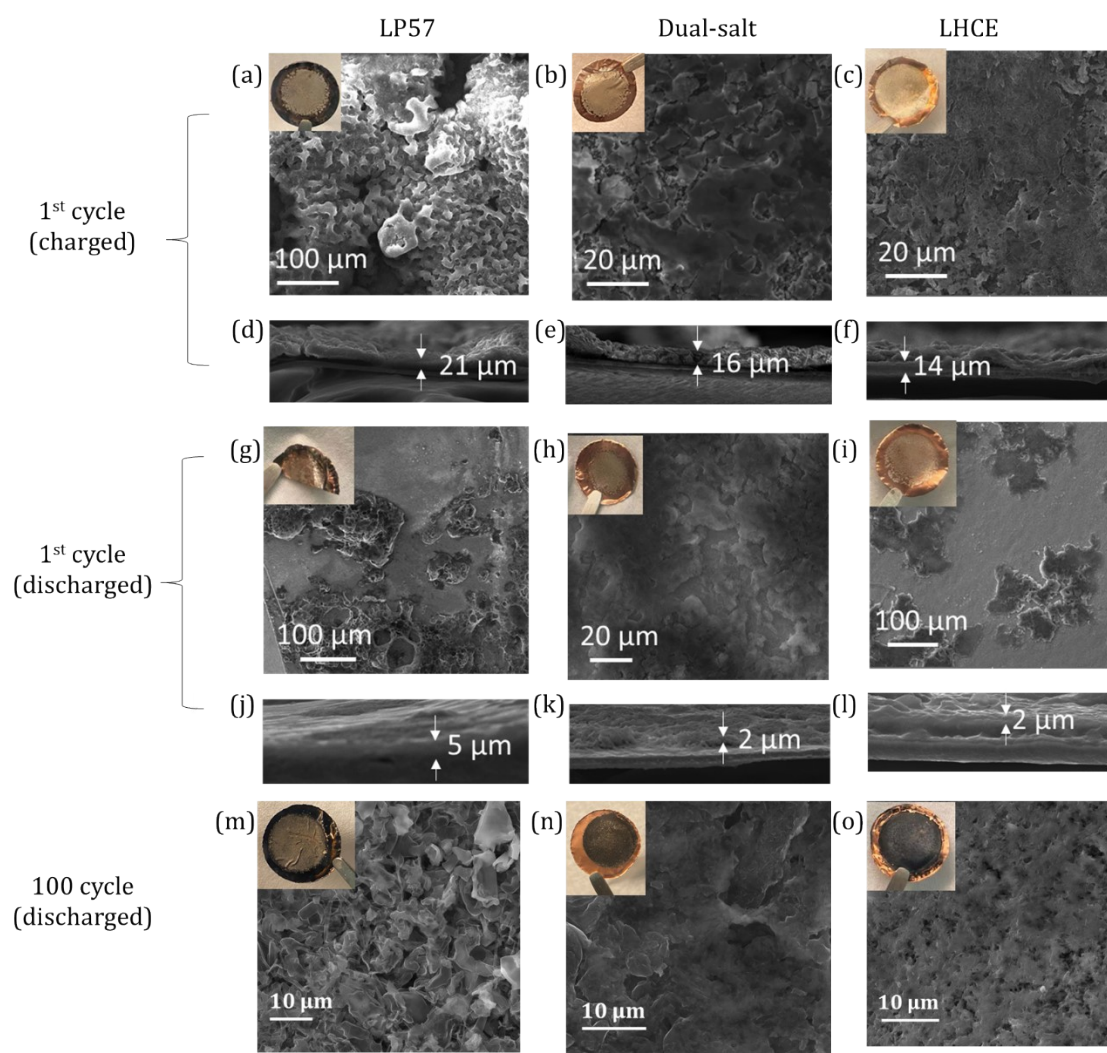


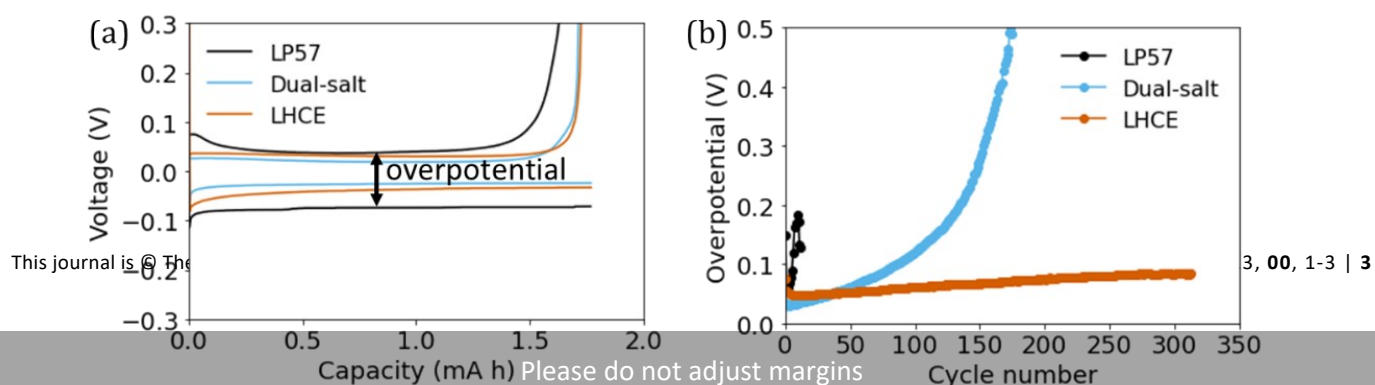
Fig. S3 Scanning electron microscope images of Cu foil taken from anode-free cells at (a-f) the charged status in the first cycle, (g-l) the discharge status in the first cycle, and (m-o) the discharged status after 100 cycles. A picture of the Cu foil with plated Li is inserted in each SEM image.

### Theoretical thickness of the plated Li on Cu foil

The loading of the cathode electrode in this study is  $2 \text{ mAh cm}^{-2}$ . If the Li is uniformly packed on the Cu foil with a porosity of zero, the thickness can be calculated using the following formula,

$$d = \frac{C_{\text{loading}}}{C_{\text{Li}} \cdot \rho_{\text{Li}} \cdot A}$$

where  $C_{\text{loading}}$  is the loading of the cathode electrode that is  $2 \text{ mAh cm}^{-2}$  here,  $C_{\text{Li}}$  is the theoretical capacity of Li that is  $3860 \text{ mAh g}^{-1}$ ,  $\rho_{\text{Li}}$  is the density of Li that is  $0.534 \text{ g cm}^{-3}$ , and  $A$  is the unit area. Substituting these values to the formula above gives a thickness of  $9.7 \mu\text{m}$ .



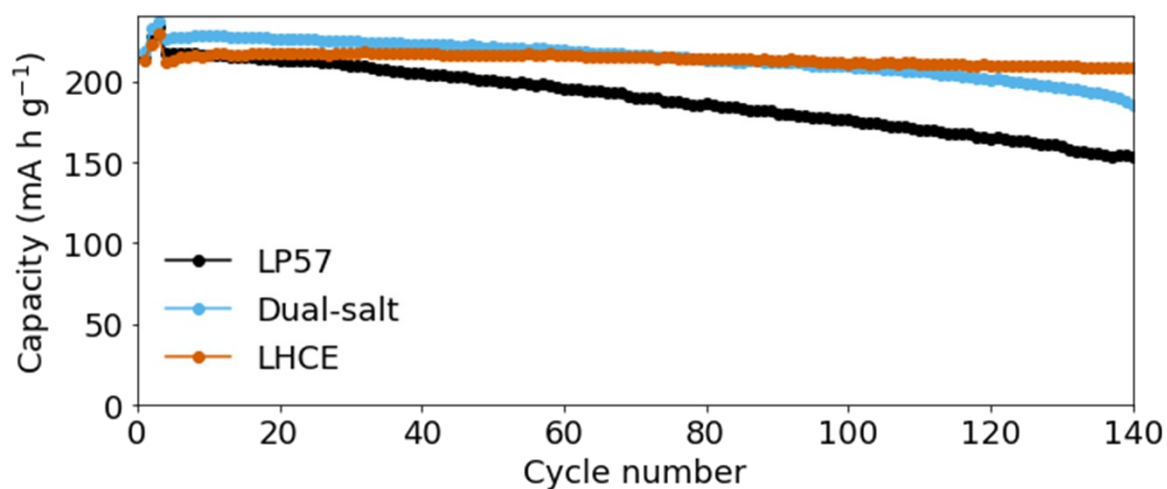


Fig. S5 Electrochemical performances of three electrolytes tested in Li|NMCAM coin cells. Cells were cycled between 2.8 to 4.4 V at C/3.

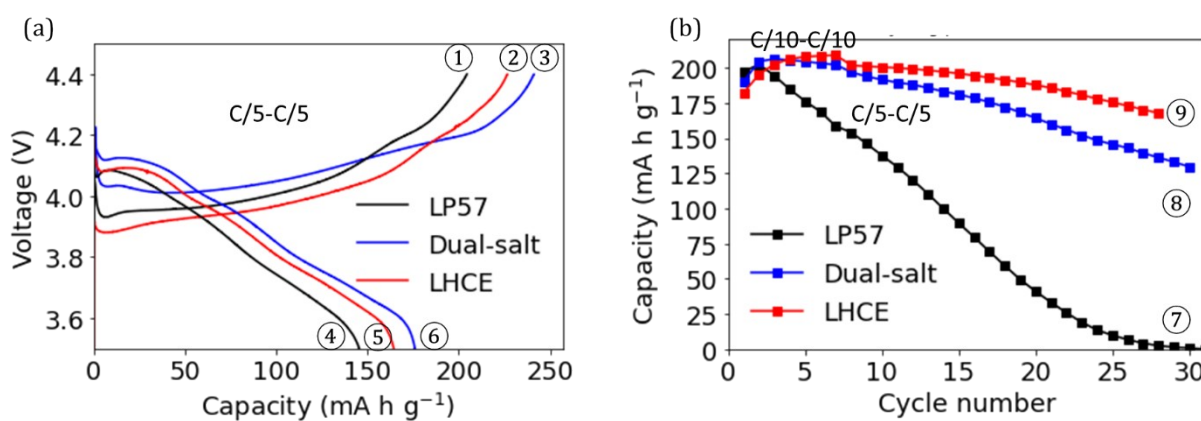
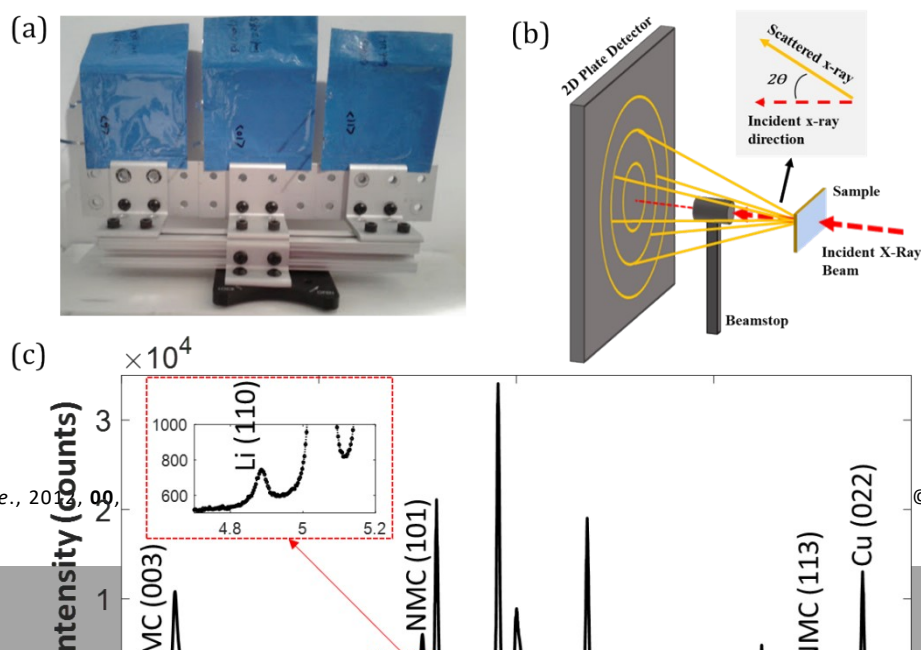
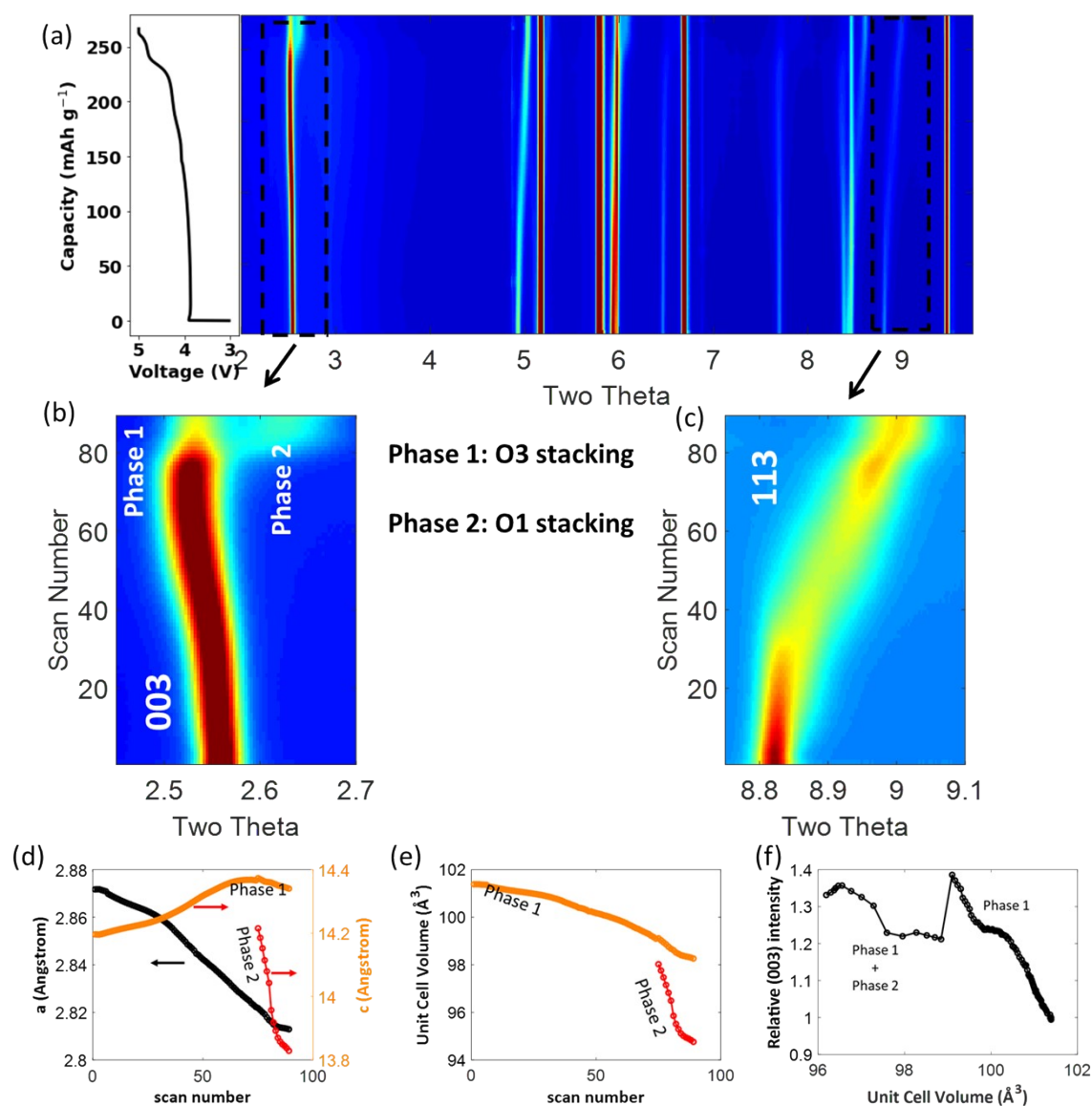
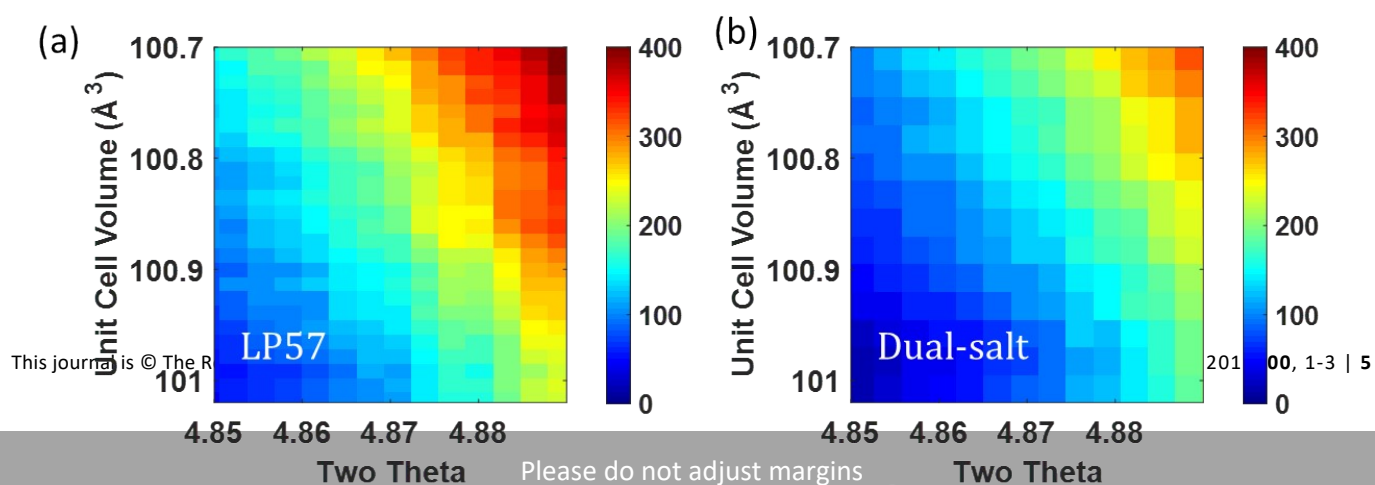


Fig. S6 Electrochemical performances of the XRD-mapping anode-free pouch cells. Nine samples were prepared for the experiment considering the availability of the beamtime. (a) Charge and discharge curves in the first formation cycle conducted at Argonne National Laboratory (ANL). Three charged cells and three discharged cells were obtained, as labelled by ①-⑥. (b) Cycling performances of three anode-free pouch cells conducted at UT Austin Lab. Three aged cells (⑦-⑨) were obtained and shipped to the Advanced Photon Sources (APS) at ANL for the XRD mapping study.





**Fig. S8** Operando XRD measurement of a NMCAM|Li half cell. (a) Evolution of the XRD pattern during charging. The (003) and (113) peaks of NMCAM are highlighted in (b) and (c). (d) Evolution of the fitted lattice parameters based on the (003) peak and the (113) peaks. (e) Evolution of the unit cell volume during charging. (f) Relationship between the (003) peak intensity and the unit cell volume of the NMCAM.





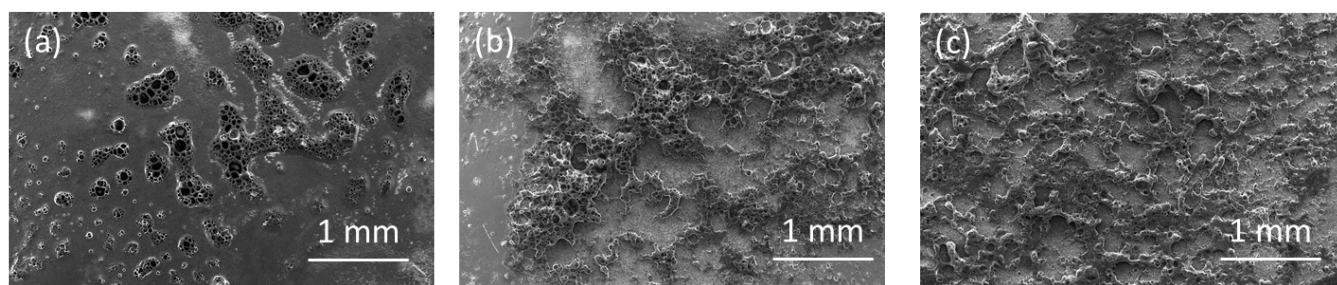


**Fig. S10** Morphology of Li plated on Cu anode with the LP57 electrolyte. The plating time is (a) 5 min, (b) 10 min, and (c) 15 min with a current density of  $1 \text{ mA cm}^{-2}$ .

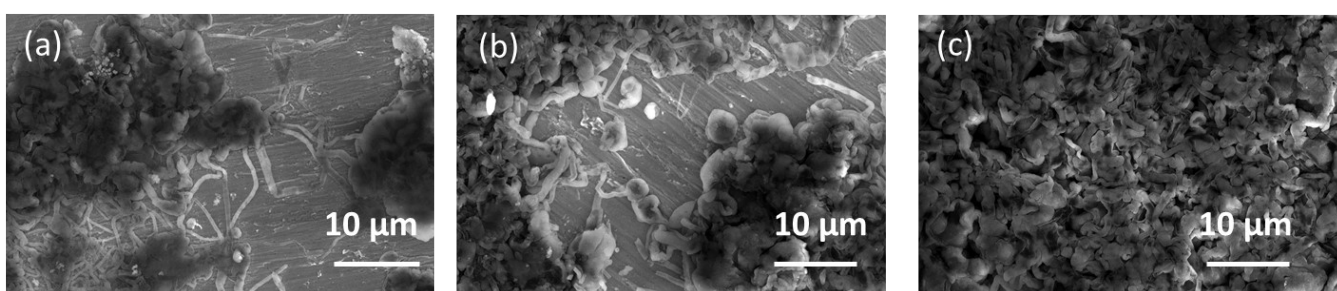


**Fig. S11** Morphology of Li plated on Cu anode with the LHCE electrolyte. The plating time is (a) 5 min, (b) 10 min, and (c) 15 min with a current density of  $1 \text{ mA cm}^{-2}$ .

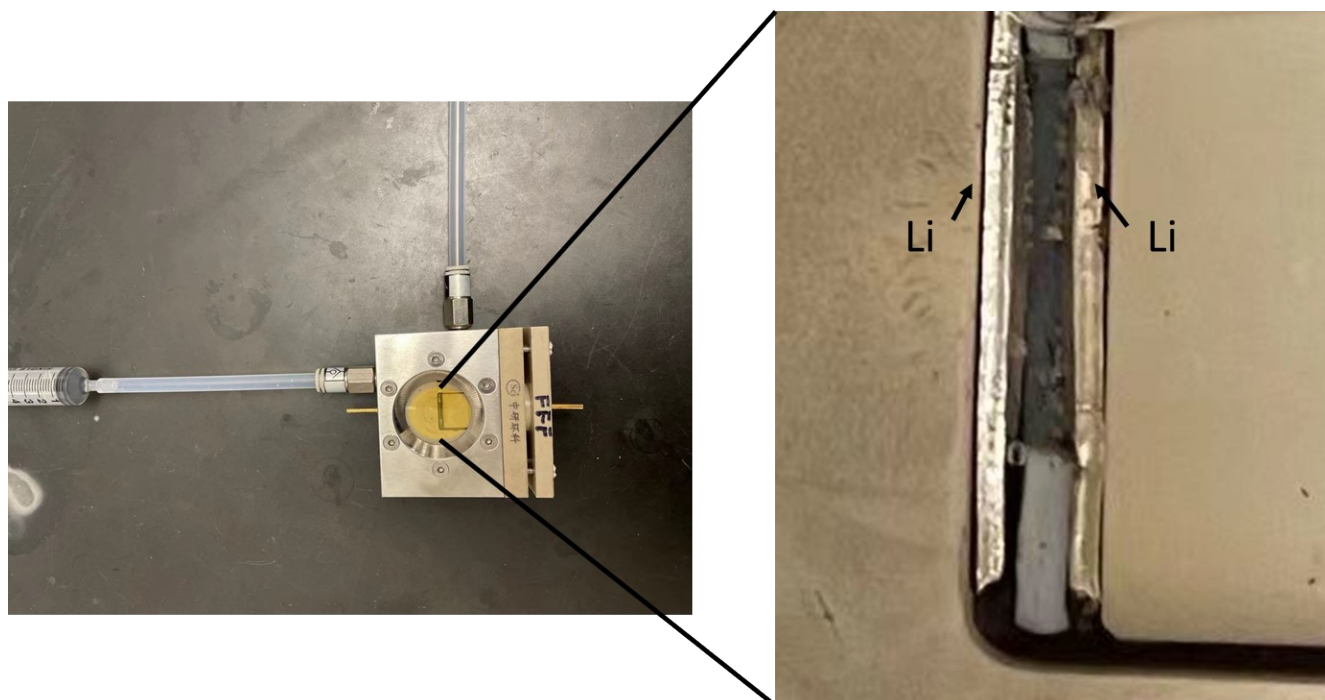


**Fig. S12** An optical cell that can be used to visualize the growth process of Li with different electrolytes.

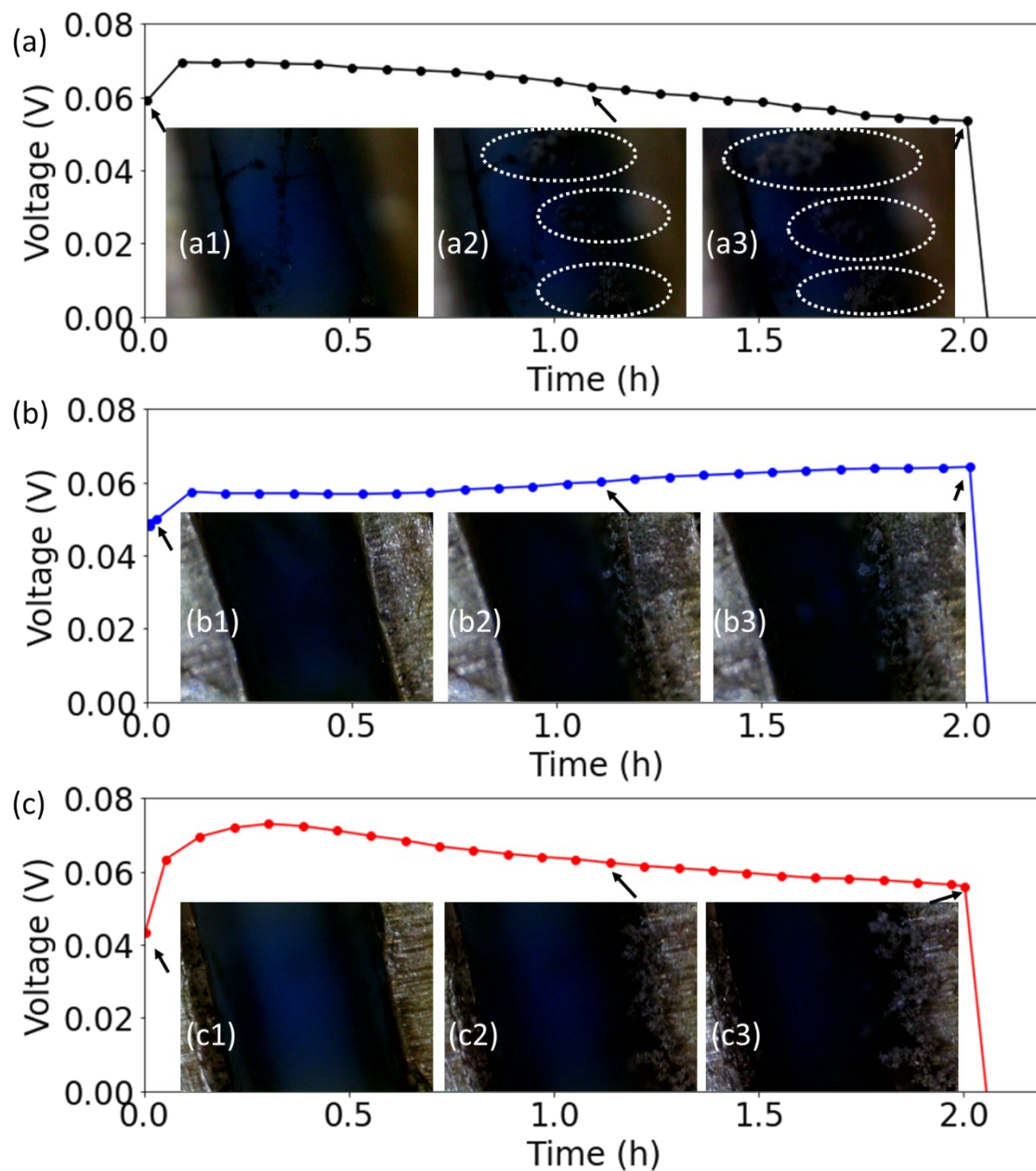


**Fig. S13** Li plating process in (a) the LP57 electrolyte, (b) dual-salt electrolyte, and (c) LHCE electrolyte measured by an optical Li|Li symmetric cell. The cell is tested at  $1 \text{ mA cm}^{-2}$  and  $2 \text{ mAh cm}^{-2}$ . The inserted images show the cross-section of the Li|Li cell at different test times. The Li plating and stripping processes are also shown in the supporting videos.

**Table S1** Recent experimental efforts on characterizing the crystallinity of electrochemically deposited Li in different electrolytes

Refs	Research group	Electrolytes	Main finding regarding Li crystallinity	Techniques
1	Cui et al.	1 M LiPF <sub>6</sub> in EC/DEC (1:1 w/w)	Li dendrites grow along the (111) (preferred), (110), or (211) direction	Cryo-TEM
2	Archer et al.	2 M LiFSI and 0.5 M LiNO <sub>3</sub> in DOL	During Li plating, Li crystallinity gradually transfers from (200) to (110) crystal facets	XRD
3	Zhang et al.	1 M LiFSI in DME/TFEO (1:9 w/w)	Only crystalline Li is identified, and it grows along (110) direction	Cryo-TEM
4	Meng et al.	1 M LiPF <sub>6</sub> in EC/EMC (1:1 w/w)	Observed amorphous Li during short plating time (5 min at 0.5 mA cm <sup>-2</sup> )	Cryo-TEM
5	Meng et al.	1 M LiPF <sub>6</sub> in EC/EMC (1:1 w/w); LiFSI in DME and TTE (1:1.2:3 by mol)	The advanced electrolyte is in favor of forming amorphous Li deposits, while the crystalline ones dominate in the conventional electrolyte	Cryo-TEM

## References

1. Y. Li, Y. Li, A. Pei, K. Yan, Y. Sun, C. L. Wu, L. M. Joubert, R. Chin, A. L. Koh, Y. Yu, J. Perrino, B. Butz, S. Chu and Y. Cui, *SCIENCE*, 2017, 358, 506-510.
2. Q. Zhao, Y. Deng, N. W. Utomo, J. Zheng, P. Biswal, J. Yin and L. A. Archer, *NAT COMMUN*, 2021, 12.
3. X. Cao, X. Ren, L. Zou, M. H. Engelhard, W. Huang, H. Wang, B. E. Matthews, H. Lee, C. Niu, B. W. Arey, Y. Cui, C. Wang, J. Xiao, J. Liu, W. Xu and J. Zhang, *NAT ENERGY*, 2019, 4, 796-805.
4. X. Wang, M. Zhang, J. Alvarado, S. Wang, M. Sina, B. Lu, J. Bouwer, W. Xu, J. Xiao, J. Zhang, J. Liu and Y. S. Meng, *NANO LETT*, 2017, 17, 7606-7612.
5. X. Wang, G. Pawar, Y. Li, X. Ren, M. Zhang, B. Lu, A. Banerjee, P. Liu, E. J. Dufek, J. Zhang, J. Xiao, J. Liu, Y. S. Meng and B. Liaw, *NAT MATER*, 2020, 19, 1339-1345.